Direct Evidence for Octupole Deformation in ^{146}Ba and the Origin of Large E1 Moment Variations in Reflection-Asymmetric Nuclei

B. Bucher *et al.*

Direct Evidence for Octupole Deformation in ^{146}Ba and the Origin of Large $E1$ Moment Variations in Reflection-Asymmetric Nuclei

B. Bucher,[1, 2, *] S. Zhu,[3, †] C. Y. Wu,[1] R. V. F. Janssens,[3] R. N. Bernard,[4] L. M. Robledo,[4] T. R. Rodríguez,[4]
D. Cline,[5] A. B. Hayes,[5] A. D. Ayangeakaa,[3] M. Q. Buckner,[1] C. M. Campbell,[6] M. P. Carpenter,[3] J. A. Clark,[3]
H. L. Crawford,[6] H. M. David,[3, ‡] C. Dickerson,[3] J. Harker,[3, 7] C. R. Hoffman,[3] B. P. Kay,[3] F. G. Kondev,[3]
T. Lauritsen,[3] A. O. Macchiavelli,[6] R. C. Pardo,[3] G. Savard,[3] D. Seweryniak,[3] and R. Vondrasek[3]

[1]*Lawrence Livermore National Laboratory, Livermore, California 94550, USA*
[2]*Idaho National Laboratory, Idaho Falls, Idaho 83415, USA*
[3]*Argonne National Laboratory, Argonne, Illinois 60439, USA*
[4]*Departamento de Física Teórica, Universidad Autónoma de Madrid, E-28049 Madrid, Spain*
[5]*University of Rochester, Rochester, New York 14627, USA*
[6]*Lawrence Berkeley National Laboratory, Berkeley, California 94720, USA*
[7]*University of Maryland, College Park, Maryland 20742, USA*

Despite the more than one order of magnitude difference between the measured dipole moments in ^{144}Ba and ^{146}Ba, the strength of the octupole correlations in ^{146}Ba are found to be as strong as those in ^{144}Ba with a similarly large value of $B(E3; 3^- \to 0^+)$ determined as $48(^{+21}_{-29})$ W.u. The new results not only establish unambiguously the presence of a region of octupole deformation centered on these neutron-rich Ba isotopes, but also manifest the dependence of the electric dipole moments on the occupancy of different neutron orbitals in nuclei with enhanced octupole strength, as revealed by fully microscopic calculations.

Unlike the electrons in atoms, protons and neutrons are closely bound together in nuclei by the strong nuclear force, occupying quantum levels that can result in different nuclear shapes because of sizeable long range multipole-multipole interactions. The studies of these shapes, and of the associated nuclear moments, facilitate our understanding of the origin of simple patterns in such complex quantum many-body systems. Certain isotopes are thought to develop octupole deformation due to strong octupole-octupole interactions present when both types of valence nucleons occupy pairs of single-particle orbitals near the Fermi surface with orbital (ℓ) and total (j) angular momenta differing by $3\hbar$ [1]. There is now experimental evidence to suggest that nuclei with a low-lying negative-parity band of states interleaved with the ground-state positive-parity band and linked by fast $E1$ transitions between the two sequences result from strong octupole correlations. However, because $E3$ transitions are fundamentally hindered in the electromagnetic decay of nuclear states when competing with $E1$ and $E2$ transitions, the presence of strong octupole correlations is often inferred from the observation of large $E1$ transition probabilities. The latter are related to the intrinsic electric dipole moment and are typically obtained from $E1/E2$ intensity ratios, with the $E2$ transition probabilities then being estimated from lifetime measurements of low-spin states or from systematics. A direct experimental determination of the electric octupole moment requires the use of the Coulomb excitation process for the nuclei of interest.

The neutron-deficient radium isotopes around ^{224}Ra and the neutron-rich barium isotopes centered at ^{146}Ba have been predicted to belong to the two regions with the strongest octupole correlations [2]. However, large fluctuations, by as much as two orders of magnitude for a given spin, in the value of the intrinsic electric dipole moment have been well documented in these two regions [1, 3], even though other spectroscopic features; i.e., negative-parity bands located at comparably low excitation energies, strongly suggest the presence of similar octupole strengths. Classically, octupole-deformed nuclei should be characterized by large electric dipole moments proportional to the strength of the octupole correlations [4, 5] because of the redistribution of the mass and charge of the protons and neutrons. Interestingly, in the radium isotopes, a minimum occurs in the value of the intrinsic electric dipole moment for ^{224}Ra, but the magnitude of octupole strength in this nucleus, as recently quantified through Coulomb excitation with a ^{224}Ra radioactive beam, is one of the largest in the region [6]. Neutron-rich barium nuclei form another interesting set in terms of studying the relationship between the intrinsic electric dipole and octupole moments [1, 7, 8]. Specifically, between ^{144}Ba$_{88}$ and ^{146}Ba$_{90}$, the electric dipole moments are observed to drop suddenly by more than an order of magnitude [7–9], but the value quickly returns to an enhanced level in ^{148}Ba$_{92}$ [9]. Furthermore, it has been pointed out in Ref. [9] that the octupole strength in ^{146}Ba may in fact be quenched as this could account for the presence of a particle alignment at moderate angular momentum $(I^\pi \sim 12^+)$ in the ground-state band. Clarification of these issues requires a direct measurement of the $E3$ strength in this nucleus, a challenge until recently because of its short half-life $(T_{1/2} = 2.2$ s [10]).

Despite the many experimental challenges associated with measurements of the electric octupole moments in these nuclei, there is also additional motivation in fundamental physics to understand the relation between the intrinsic electric dipole and octupole moments: The existence of an atomic electric dipole moment (EDM) has important implications for CP-violation in the early universe that could possibly be responsible for the observed asymmetry between matter and anti-matter [11], herewith signifying new physics beyond the Standard Model [12]. In diamagnetic atoms, a measureable EDM could be induced by the so-called Schiff moment, a quantity that can be enlarged by orders of magnitude by a sizeable octupole moment and is sensitive to details of the charge distribution [13, 14]. Moreover, the contribution of the nuclear intrinsic electric dipole moment to the Schiff moment is not negligible [14]. Hence, it is important to recognize the origin and magnitude of nuclear intrinsic moments, especially the electric dipole moment as it is closely associated with the nuclear mass and charge distributions. An accurate estimate of Schiff moments for different nuclei is required to evaluate the precision of calculations of this quantity and to compare the limits on P and T violation reported by various experiments involving them.

To determine the octupole strength in ^{146}Ba, a Coulomb excitation experiment was performed similar to the one carried out recently for ^{144}Ba [15]. The beam of ^{146}Ba ions was produced from ^{252}Cf fission in the CARIBU facility [16, 17] along with the isobaric contaminants ^{146}La and ^{146}Ce, and was charge bred to $q=28^+$. The $A=146$ beam was accelerated through the ATLAS accelerator to 659 MeV and was focused onto a 1.1 mg/cm^2 ^{208}Pb target (99.86% enriched). The average ^{146}Ba beam intensity was 3×10^3 ions per second over 12 days. Additional stable contaminants (with the same A/q) included ^{94}Mo^{18+}, ^{94}Zr^{18+}, ^{120}Sn^{23+}, ^{193}Ir^{37+}, and ^{198}Hg^{38+}, but all were readily separated from the $A=146$ beam, based on time-of-flight (TOF) and scattering angle data recorded in the CHICO2 heavy-ion counter [18] (Fig. 1). This allowed for a clean $A=146$ γ-ray spectrum resulting from Coulomb excitation (Fig. 2).

In the spectrum of Fig. 2, measured with the GRETINA γ-ray tracking array [19], several transitions from ^{146}Ba are apparent, especially those belonging to positive-parity levels in the ground-state band which are excited (and decay) by $E2$ transitions. The negative-parity levels are populated less frequently, but the excitation occurs predominantly through $E3$ transitions and their decay yields provide a measurement of the corresponding $E3$ matrix elements.

The γ-ray yields were extracted for two separate scattering angle (θ) ranges: 30°–40° and 40°–75°. At lower angles, it is difficult to isolate the $A=146$ ions from other beam contaminants in the TOF spectrum while, at higher θ values, statistics are insufficient (the cross sections fall
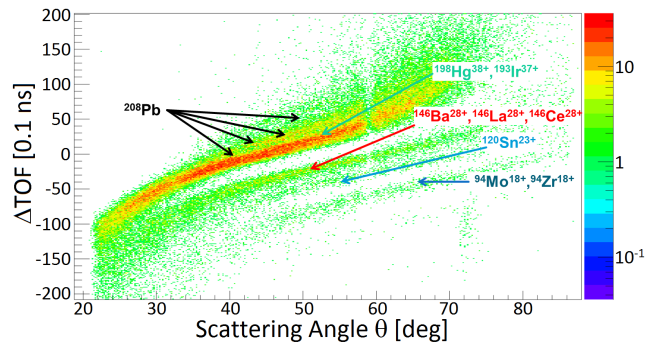

FIG. 1. (Color) TOF vs. scattering angle recorded by CHICO2 in coincidence with a γ ray observed in GRETINA. The $A=146$ group is readily distinguished from the stable beam contaminants.
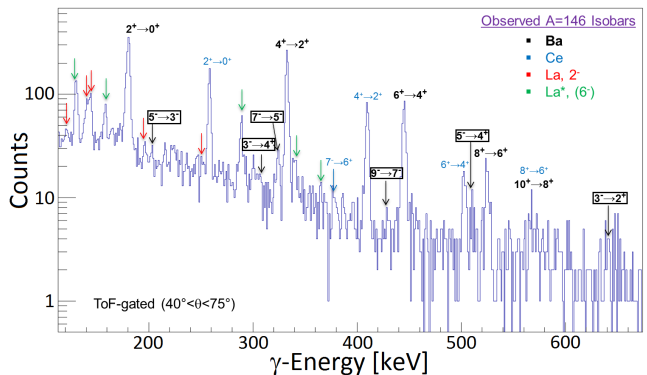

FIG. 2. (Color online) The coincident γ-ray spectrum obtained by gating on the $A=146$ group in the CHICO2 TOF spectrum (Fig. 1). Many ^{146}Ba transitions are seen along with lines from the radioactive isobaric contaminants that were also produced in CARIBU.

off with the $1/\sin^4(\frac{\theta}{2})$ Rutherford angular dependence). The data for each set of angles were analyzed with the Coulomb excitation least-squares search code, GOSIA [20]. Yields were determined for levels up to $10\hbar$ in the ground-state band and $9\hbar$ in the negative-parity sequence. The energies of all observed γ rays, along with several branching ratios and level lifetimes, were known from previous works [7–10]. The latter information proved useful for constraining the GOSIA fit. The sets of $E1$, $E2$, and $E3$ matrix elements between levels with no previously known lifetimes were coupled according to the rigid-rotor prescription [21] governed by the individual intrinsic $E\lambda$ moments (see also Refs. [7, 15, 22]). Once the χ^2 minimum was found, the rigid-rotor constraint was removed to properly determine the associated uncertainties, including correlations between matrix elements. In most cases, the uncertainty was primarily limited by the lack of statistics in the measured yields due to the low radioactive beam intensity.

As anticipated, the extracted $E1$ matrix elements did not display much sensitivity to the data; as mentioned

TABLE I. The experimental $|\langle I_f^\pi \| \hat{M}_\lambda \| I_i^\pi \rangle|$ matrix elements $(e \cdot b^{\lambda/2})$ based on the GOSIA fit along with new symmetry-conserving configuration-mixing calculations (see text and Ref. [24] for details).

$I_i^\pi \to I_f^\pi$	$E\lambda$	Exp.	SCCM
$0^+ \to 1^-$	$E1$	$0.000223(^{10}_{-8})$ [a]	0.00474
$1^- \to 3^-$	$E2$	1.2(5)	1.6
$0^+ \to 2^+$	$E2$	$1.17(2)$ [a]	1.14
$2^+ \to 4^+$	$E2$	1.97(14)	1.90
$4^+ \to 6^+$	$E2$	$2.35(^{+20}_{-24})$	2.43
$6^+ \to 8^+$	$E2$	$2.17(^{+65}_{-33})$	2.90
$0^+ \to 3^-$	$E3$	$0.65(^{+14}_{-20})$	0.54
$2^+ \to 5^-$	$E3$	$1.01(^{+61}_{-20})$	0.87
$4^+ \to 7^-$	$E3$	$1.25(^{+85}_{-34})$	1.11
$6^+ \to 9^-$	$E3$	$1.5(^{+8}_{-12})$	

[a] primarily determined by previous lifetime and/or branching ratio data [10]

above, the dipole strength was known to be small from earlier work [7–9] and, in fact, the only observed γ rays from $E1$ decays in the present measurement came from the 3^- and 5^- states. Moreover, the relative sign between the intrinsic $E1$ and $E3$ moments was found to also be insensitive to the data. On the other hand, a number of new $E2$ and $E3$ matrix elements were well-determined from the data (Table I).

The most significant result obtained here is the ground-state $E3$ matrix element $|\langle 3_1^- \| \hat{M}_{E3} \| 0_1^+ \rangle|$; it is determined to be $0.65(^{+14}_{-20})\ eb^{3/2}$ and reflects the amplitude of octupole deformation present in the ground state [1]. This value corresponds to a $B(E3; 3^- \to 0^+)$ reduced transition probability of $48(^{+21}_{-29})$ W.u. which is essentially the same as the value of $48(^{+25}_{-34})$ W.u. reported recently for ^{144}Ba [15]. This new result supports the long standing prediction that ^{146}Ba is indeed one of the isotopes with strong octupole collectivity [23].

The persistence of this strong collectivity between ^{144}Ba$_{88}$ and ^{146}Ba$_{90}$ confirms that the drastic reduction in electric dipole moment between the two isotopes is not the result of quenched octupole strength, as suggested by the high-spin behavior of ^{146}Ba. The sudden band alignments in ^{146}Ba pointed out in Ref. [9], are then most likely the result of a crossing between yrast and yrare bands predicted in this mass region sometime ago [25, 26]. It should be noted that alternative explanations have also been proposed. These include a transition to a more reflection-symmetric shape at moderate spin [27], and a description in terms of a condensate of rotationally-aligned octupole phonons [28, 29]. Concerning the latter, however, it should be mentioned that while the interleaved sequences of opposite parity are consistent with the proposed picture, the absence of strong $E1$ linking transitions associated with multi-octupole phonon exci-

tations at higher spins is not.

Over the past three decades, extensive theoretical efforts have been devoted to understanding the variation of the $E1$ transition strengths observed in nuclei near ^{146}Ba and ^{224}Ra [30–38]. It is generally believed that the observations are the result of the relation between octupole collectivity and the non-uniform distribution of protons and neutrons. This was first shown within the framework of a macroscopic-microscopic approach where the experimental $E1$ transition strengths could be described [30, 34]. Early self-consistent Hartree-Fock-Bogoliubov (HFB) calculations with the Gogny interaction were also able to reproduce the very low values of the dipole moment D_0 in ^{224}Ra and ^{146}Ba [33, 35]. However, all of these models predicted that the nuclei under study are reflection-asymmetric, and argued that this is at the core of the observed variations. Thus, the recently measured strong octupole collectivity in ^{144}Ba [15] and ^{146}Ba (Table I) provides an important validation of this interpretation.

More recently, microscopic self-consistent methods have been improved by including beyond-mean-field correlations. These developments provide an explanation of the microscopic origin of octupole collectivity and study the impact of octupole correlations on both ground-state properties and electromagnetic transitions. To explore in ^{146}Ba this phenomenon of a strong octupole collectivity accompanied by a much reduced electric dipole moment, a theoretical model based on mean field HFB intrinsic wave functions has been used with a symmetry-conserving configuration-mixing method (SCCM). The model assumes that only the axially symmetric quadrupole (Q_{20}) and octupole (Q_{30}) degrees of freedom are relevant (collectively referred to as $\mathbf{Q}$). A set of constrained HFB states $|\mathbf{Q}\rangle$, subsequently projected onto good angular momentum, parity and particle number (the corresponding states are denoted as $|\Phi^{J,\pi}(\mathbf{Q})\rangle$) is used as a variational subspace. Linear combinations of the above states $|\Psi_\sigma^{J,\pi}\rangle = \sum_{\mathbf{Q}} f_\sigma^{J,\pi}(\mathbf{Q})|\Phi^{J,\pi}(\mathbf{Q})\rangle$ are used in the spirit of the generator coordinate method (GCM) to obtain the low-lying collective spectrum (see Ref. [24] for a recent account and an application to ^{144}Ba). The interaction generating the intrinsic states is the well-known Gogny D1S force [39]. The physics of the low-lying quadrupole and octupole states is contained in the collective amplitudes $F_\sigma^{J,\pi}(\mathbf{Q})$ defined in Eq (5) of Ref. [24] in terms of the GCM amplitudes $f_\sigma^{J,\pi}(\mathbf{Q})$ (the latter are obtained by solving the Hill-Wheeler (HW) equations of the GCM).

The HFB potential energy surface (PES) as a function of the deformation parameters β_2 and β_3 is given in Fig 3 for ^{146}Ba. Note that the potential energy is symmetric under the change of sign of β_3 due to the parity symmetry of the nuclear interaction. A reflection-asymmetric, absolute minimum is obtained at $\beta_2 = 0.21$ and $\beta_3 = \pm 0.1$. The shape of the $F^{J,\pi}$ collective amplitudes is mainly
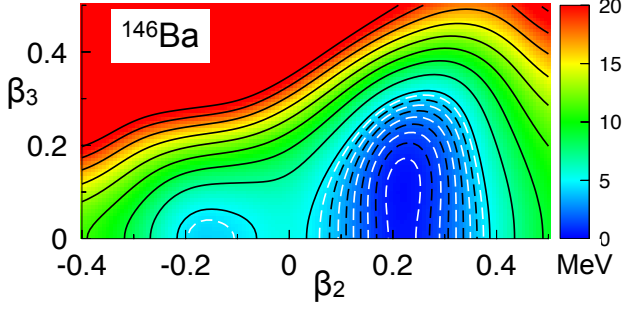
FIG. 3. (Color online) The HFB potential energy surface. Axial quadrupole (β_2) and octupole (β_3) deformation parameters are defined as $\beta_\lambda \equiv 4\pi\langle\mathbf{q}|r^\lambda Y_{\lambda 0}|\mathbf{q}\rangle/(3r_0^\lambda A^{\lambda/3+1})$ with $r_0 = 1.2$ fm and A being the mass number. Dashed (solid) contour lines are separated by 0.5 MeV (2.0 MeV).

FIG. 4. (color online) Collective amplitudes corresponding to ^{144}Ba (left), ^{146}Ba (middle), and ^{148}Ba (right).

driven by the intrinsic potential energy surface. As a consequence, the $F^{J,\pi}$ amplitudes for ^{146}Ba are concentrated around those minima as seen in Fig 4 where they are compared with those for ^{144}Ba and ^{148}Ba. In the three nuclei, the 1^- and 0^+ collective amplitudes have a very large overlap, characteristic of strong octupole correlations. The energy of the 1^- state is well-reproduced, however the ground-state and negative-parity sequences are characterized by a smaller moment of inertia than observed, due to limitations discussed in Ref. [24].

The electromagnetic transition strengths have been computed without invoking effective charges or uncontrolled approximations. The calculated values are compared with the experimental data in Table I. There is fair agreement between the calculated and measured $E\lambda$ matrix elements, including the strong $B(E3)$ strengths between the 3^- and 0^+ and the much quenched $E1$ between the 1^- and 0^+ states. In the present microscopic framework, the $B(E1)$ transition strength is proportional to the square of the overlap of the dipole operator between the initial 1^- and final 0^+ states. There are two basic ingredients entering the required overlap (see Eq (4) of Ref. [24]). One is the structure of the collective wave functions $F_\sigma^{J,\pi}(\mathbf{Q})$, and the other is the overlap between the projected intrinsic states $|\Phi^{J,\pi}(\mathbf{Q})\rangle$. Because the values of $F_\sigma^{J,\pi}(\mathbf{Q})$, as shown in Fig 4, exhibit little variation with neutron number in the three Ba isotopes, the sudden drop of $B(E1)$ in ^{146}Ba has to be associated with the overlap of the dipole operator between the projected intrinsic states $|\Phi^{J,\pi}(\mathbf{Q})\rangle$. Specifically, the calculations indicate that the dipole moment changes from positive values in ^{144}Ba, to nearly zero values in ^{146}Ba, and finally to negative values in ^{148}Ba. Hence, the changes in $E1$ strengths with neutron number are associated with changes in the intrinsic dipole moment linked to the evolving mean field. A similar conclusion was reached in Ref. [35].

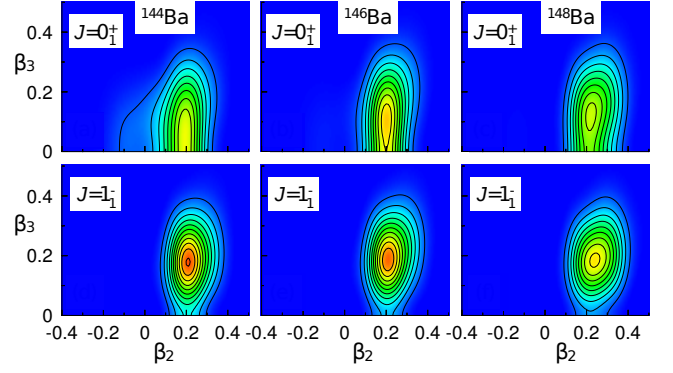The behavior of the dipole moment with neutron num-
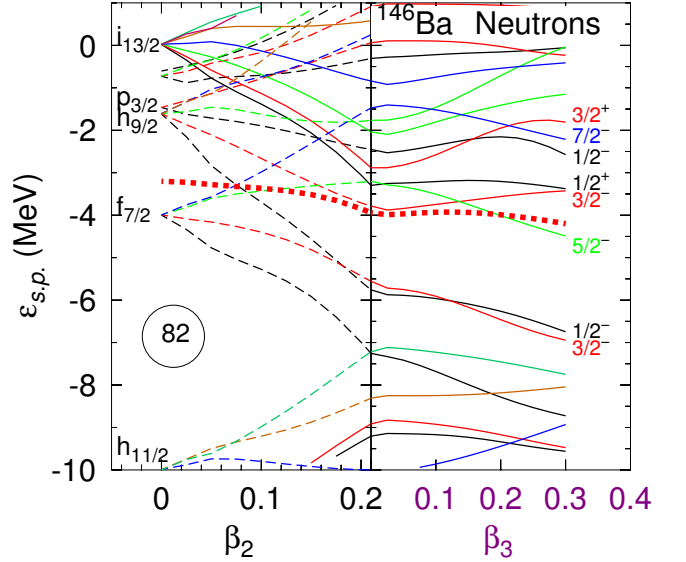

FIG. 5. (Color) Neutron single-particle energies (SPE) as a function of β_2 (left) and as a function of β_3 (right) for ^{146}Ba. The right panel is calculated with a constant value of $\beta_2=0.2$ (ground-state value) starting with $\beta_3=0$ at the central vertical axis. A thick dotted line shows the Fermi level. The SPE as a function of β_2 is used to justify the spherical orbital assignments and parities of the relevant neutron orbitals (see text for details).

ber in these Ba isotopes can further be traced back to the occupation of specific single-particle states near the Fermi surface. Considering the evolution of the single-particle energies with β_3 in Fig 5, three neutron orbitals are of interest with K^π quantum numbers $3/2^-$, $5/2^-$ and $1/2^+$. These are of $h_{9/2}$, $f_{7/2}$, and $i_{13/2}$ spherical parentage, respectively. The three states are empty in ^{144}Ba, but have significant respective occupancies of $v^2 = 0.4$, $v^2 = 0.27$, and $v^2 = 0.20$ in ^{146}Ba. As visualized in Fig. 4 of Ref. [35], their occupation results in a contribution to the dipole moment which almost cancels that by the protons. As the occupancies increase further with two additional neutrons in ^{148}Ba, the (total) dipole

moment changes sign and returns to a sizeable value.

To summarize, the $E3$ strength in short-lived ^{146}Ba was measured directly by multi-step Coulomb excitation with GRETINA and CHICO2. The longstanding prediction of an enhanced octupole collectivity was verified. The data also provide firm experimental evidence that the large drop of $B(E1)$ value is not the result of quenched octupole collectivity in ^{146}Ba. Such a collectivity is well-reproduced by the SCCM model with the Gogny energy density functional, and the variation in $E1$ strength between isotopes is associated with changes in the neutron occupancy of high-j, low-K orbitals located near the Fermi surface. The present results help validate the general character of the microscopic origin of large variations in electric dipole moments in the reflection-asymmetric nuclear potential, and they represent an important confirmation of such effects in the Ba region of neutron-rich nuclei.

---

* brian.bucher@inl.gov

† zhu@anl.gov

‡ Present address: GSI Helmholtzzentrum für Schwerionenforschung, 64291 Darmstadt, Germany

[1] P. A. Butler and W. Nazarewicz, Rev. Mod. Phys. **68**, 349 (1996).

[2] P. A. Butler, J. Phys. G **43**, 073002 (2016).

[3] I. Ahmad and P. A. Butler, Annu. Rev. Nucl. Part. Sci. **43**, 71 (1993).

[4] B. M. Strutinsky, Sov. J. At. Energy **1**, 611 (1956).

[5] A. Bohr and B. R. Mottelson, Nucl. Phys. **4**, 529 (1957).

[6] L. P. Gaffney *et al.*, Nature (London) **497**, 199 (2013).

[7] W. R. Phillips, I. Ahmad, H. Emling, R. Holzmann, R. V. F. Janssens, T.-L. Khoo, and M. W. Drigert, Phys. Rev. Lett. **57**, 3257 (1986).

[8] H. Mach, W. Nazarewicz, D. Kusnezov, M. Moszyński, B. Fogelberg, M. Hellstrom, L. Spanier, R. L. Gill, R. F. Casten, and A. Wolf, Phys. Rev. C **41**, R2469 (1990).

[9] W. Urban *et al.*, Nucl. Phys. A **613**, 107 (1997).

[10] L. K. Peker and J. K. Tuli, Nucl. Data Sheets **82**, 187 (1997).

[11] C. P. Liu, M. J. Ramsey-Musolf, W. C. Haxton, R. G. E. Timmermans, and A. E. L. Dieperink, Phys. Rev. C **76**, 035503 (2007).

[12] J. Engel, M. J. Ramsey-Musolf, and U. van Kolck, Prog. Part. Nucl. Phys. **71**, 21 (2013).

[13] N. Auerbach, V. V. Flambaum, and V. Spevak, Phys. Rev. Lett. **76**, 4316 (1996).

[14] V. Spevak, N. Auerbach, and V. V. Flambaum, Phys. Rev. C **56**, 1357 (1997).

[15] B. Bucher *et al.*, Phys. Rev. Lett. **116**, 112503 (2016).

[16] G. Savard, S. Baker, C. Davids, A. F. Levand, E. F. Moore, R. C. Pardo, R. Vondrasek, B. J. Zabransky, and G. Zinkann, Nucl. Instrum. Methods B **266**, 4086 (2008).

[17] G. Savard, A. Levand, R. Pardo, R. Vondrasek, and B. Zabransky, JPS Conf. Proc. **6**, 010008 (2015).

[18] C. Y. Wu, D. Cline, A. Hayes, R. S. Flight, A. M. Melchionna, C. Zhou, I. Y. Lee, D. Swan, R. Fox, and J. T. Anderson, Nucl. Instrum. Methods A **814**, 6 (2016).

[19] S. Paschalis *et al.*, Nucl. Instrum. Methods A **709**, 44 (2013).

[20] T. Czosnyka, D. Cline, and C. Y. Wu, Bull. Am. Phys. Soc. **28**, 745 (1983); GOSIA user manual, http://www.pas.rochester.edu/~cline/Gosia/Gosia_Manual_20120510.pdf, accessed March 2014.

[21] A. Bohr and B. R. Mottelson, *Nuclear Structure*, Vol. 2 (W. A. Benjamin, Inc., Reading, MA, 1975).

[22] H. J. Wollersheim *et al.*, Nucl. Phys. A **556**, 261 (1993).

[23] At the time of this writing, a new evaluation on ^{146}Ba was published [40] which identifies a γ-ray transition with strong intensity connecting the 3_1^- level to the ground state. However, the details surrounding the measurement responsible for this result are not easily accessible while the corresponding $B(E3)$ is unphysically high ($\sim$1600 W.u.). The non-observation of this γ ray in Refs. [8, 9, 41, 42] is consistent with the present result.

[24] R. N. Bernard, L. M. Robledo, and T. R. Rodríguez, Phys. Rev. C **93**, 061302(R) (2016).

[25] R. Bengtsson and S. Frauendorf, Nucl. Phys. A **314**, 27 (1979).

[26] R. Bengtsson, I. Hamamoto, and B. Mottelson, Phys. Lett. B **73**, 259 (1978).

[27] W. Nazarewicz and S. L. Tabor, Phys. Rev. C **45**, 2226 (1992).

[28] S. Frauendorf, in *Proceedings of the Fifth International Conference on ICFN5*, November 4–10, 2012, Sanibel Island, Florida, USA (World Scientific, 2013) pp. 39–48.

[29] S. Frauendorf, Phys. Rev. C **77**, 021304(R) (2008).

[30] G. A. Leander, W. Nazarewicz, G. F. Bertsch, and J. Dudek, Nucl. Phys. A **453**, 58 (1986).

[31] I. Hamamoto, J. Höller, and X. Z. Zhang, Phys. Lett. B **226**, 17 (1989).

[32] L. K. Peker and J. H. Hamilton, J. Phys. G **5**, L165 (1979).

[33] J. L. Egido and L. M. Robledo, Nucl. Phys. A **494**, 85 (1989).

[34] P. A. Butler and W. Nazarewicz, Nucl. Phys. A **533**, 249 (1991).

[35] J. L. Egido and L. M. Robledo, Nucl. Phys. A **518**, 475 (1990).

[36] J. L. Egido and L. M. Robledo, Nucl. Phys. A **545**, 589 (1992).

[37] L. M. Robledo, M. Baldo, P. Schuck, and X. Viñas, Phys. Rev. C **81**, 034315 (2010).

[38] C. O. Dorso, W. D. Myers, and W. J. Swiatecki, Nucl.

Phys. A **451**, 189 (1986).

[39] J. F. Berger, M. Girod, and D. Gogny, Nucl. Phys. A **428**, 23 (1984).

[40] Yu. Khazov, A. Rodionov, and G. Shulyak, Nucl. Data Sheets **136**, 163 (2016).

[41] S. M. Scott, W. D. Hamilton, P. Hungerford, D. D. Warner, G. Jung, K. D. Wünsch, and B. Pfeiffer, J. Phys. G **6**, 1291 (1980).

[42] A. J. Mitchell *et al.*, Phys. Rev. C **93**, 014306 (2016).